RSC Advances

RSC Advances

www.rsc.org/advances

ROYAL SOCIETY OF CHEMISTRY

www.rsc.org/advances

Journal Name

ARTICLE

Graphene oxide-based fluorescence molecularly imprinted composite for recognition and separation of 2,4,6-trichlorophenol

Shuang Han [a,b], Xin Li [a,c,]*, Yuan Wang [d], Shaona Chen [a]

In this work, a multifunctional molecularly imprinted polymers (MIPs) based on CdTe quantum dots (QDs) and graphene oxide (GO) were prepared for selective recognition and separation of 2,4,6-trichlorophenol (2,4,6-TCP). GO was used to improve the adsorption capacity and sensing rate of MIPs. CdTe QDs offered a readout signal to monitor the amount of 2,4,6-TCP bound to the imprinted matrix. The molecularly imprinted shell provided analyte selectivity. The prepared composite was evaluated and characterized by scanning electron microscope, transmission electron microscopy, fluorescence spectroscopy, fluorescence microscopy, Raman spectroscopy, thermo gravimetric analysis，and X-ray diffraction analysis. MIPs were successfully applied to direct fluorescence quantification of 2,4,6-TCP. The linear relationship was from 0.2 to 40 umol L^{-1}, with a detection limit of 0.18 umol L^{-1} which provided a simple and selective sensing system for recognition of 2,4,6-TCP. Moreover, the molecularly imprinted solid phase extraction (MISPE) method followed by high performance liquid chromatography (HPLC) for detection of 2,4,6-TCP was also established. The linear relationship was from 0.02 to 2.5 umol L^{-1} with a detection limit of 0.25 ng mL^{-1}, which was more suitable to determine trace 2,4,6-TCP.

1. Introduction

Chlorophenols (CPs) are common and recalcitrant environmental pollutants, because of high toxicity, carcinogenic properties, and bioaccumulation capability[1]. They have been widely employed in different manufacturing processes, and they also result from pulp bleaching, dechlorination of drinking water and incineration processes[2]. 2,4,6-Trichlorophenol (2,4,6-TCP) is one of the most significant pollutants among CPs due to pulmonary lesions that it causes[3-5]. It has been classified as priority pollutants by the U.S. Environmental Protection Agency[6]. Therefore, highly selective separation and sensitive recognition of 2,4,6-TCP from complex samples are in great demand.

Molecular imprinting allows creation of artificial recognition sites in synthetic polymers and has received much attention[7,8]. Molecularly imprinted polymers (MIPs) display significant advantages such as high selectivity, affinity, good stability and the capability of resistance to harsh environment et al.[9,10]. Therefore, MIPs have a wide range of applications in solid-phase extraction, drug delivery, and mimicking antibodies[11-13]. Use as a novel selective sorbent for the removal of CPs from complicate matrices is one of the most advanced applications of molecular imprinting.

Quantum dots (QDs) as luminescence nanocrystals has attracted considerable attention in recent years, owing to their unique optical and electronic properties, such as sharp emission band with broad excitation, high luminescence efficiency and strong resistance to photobleaching[14,15]. Surface functionalization is important to fabricate QDs based sensors because surface modifications afford not only excellent stability of QDs but also desirable surface binding sites[16]. QDs-based MIPs sensors which can provide the source of fluorescence and improve the selectivity have attracted grate attention[17-20]. For example, Y. Lee et al. developed MIPs-capped CdTe quantum dots for selective optosensing of clenbuterol and melamine[21]. X.P. Yan et al. prefabricated MIPs by anchoring MIPs layer on the surface of Mn-doped ZnS QDs via a surface molecular imprinting process[22].

Graphene oxide (GO), with hydrophilicity, large area and unique electrical properties, should be an excellent candidate as a supported material for preparing of MIPs-based composite[23]. This form means to control templates to situate at the surface or in the proximity of the materials surface to solve the drawbacks of bulk MIPs, such as time-consuming, low binding capacity, poor site accessibility, and slow binding kinetics. Some groups have already synthesized composite materials based on the desirable merging of GO and MIPs, which make it possible to increase the adsorption capability, sensitivity and improve the binding kinetic properties of MIPs [24-27]. For example J. Ji et al. synthesized acrylamide MIPs by atom transfer radical polymerizationon GO particles, which possessed good acrylamide adsorption capacity and used to selective determine acrylamide in fried food samples. H.L. Liu

et al. prepared a ionic liquid stabilized molecularly imprinted optosensing material based on QDs and GO composites for highly selective and sensitive specific recognition of vitamin E [28,29]. These composites mostly served as electrochemical sensors or sorbents. To the best of our knowledge, merging GO and fluorescence MIPs for the applications of both fluorescence detection and molecularly imprinted solid phase extraction (MISPE) method followed by high performance liquid chromatography（HPLC）has not been reported.

In this work, the composite merging of GO and fluorescence imprinted polymers was synthesized, which involves synthesis of CdTe QDs, CdTe@SiO$_2$ deposition onto the GO surface, MIPs-functionalization onto the composite surface. This hybrid takes the advantages of high selectivity of imprinted polymers and strong fluorescence property of QDs. Moreover, owning to the use of GO, the resultant MIPs displays fast sensing rate and high adsorption capacity. MIPs were successfully applied to direct fluorescence quantification of 2,4,6-TCP and MISPE method followed by HPLC for enrichment and analysis of 2,4,6-TCP.

2. Experimental

2.1. Materials

2,4,6-Trichlorophenol（2,4,6-TCP）, thioglycollic acid, 3-aminopropyl triethoxysilane (APTES), and *p*-chlorophenol (4-CP) were obtained from Sigma-Aldrich Co. (St. Louis, MO). Tellurium powder, graphite power, CdCl$_2$·2.5H$_2$O, NaBH$_4$, ethyleneglycol dimethacylate (EDMA) and tetraethoxysilane (TEOS) were purchased from Shanghai Chemical Reagent Company (Shanghai, China). Ethanol, phenol (Phe) and azo(bis)isobutyronitrile (AIBN) were purchased from Tianjin Reagent Plant (Tianjin, China). The reagents for HPLC were at least of HPLC grade, other chemicals were analytical reagent grade.

2.2. Preparation of MIPs

Fig. 1 displays the schematic illustration of MIPs preparation. GO was prepared by modified Hummers methods [30]. Thioglycollic acid-CdTe QDs were synthesized in aqueous solution, as described in previously published procedure with minor modification[31], and then the product was mixed with 60.0 mL of ethanol and 10 mL of highly purified water, followed by the addition of 1.0 mL of ammonium hydroxide (25%) and 1.0 mL of TEOS sequentially. The mixture reacted for 24 h at room temperature under continuous stirring. Then the resultant product CdTe@SiO$_2$ was washed and dried. Silica shell was used to avoid leakage of CdTe QDs and facilitate the imprinting process.

The MIPs were synthesized as follows. At first, 0.5 g of GO was dispersed in 10 mL ethanol. After adding 1 g of CdTe@SiO$_2$, the mixture was stirred for 3 h to obtain GO-CdTe@SiO$_2$ composite. Subsequently, 2 mmol of APTES as functional monomer and 0.50 mmol of 2,4,6-TCP as template were dissolved in 80 mL of ethanol, and then fully stirred to ensure the interaction between them. At last, the obtained GO-CdTe@SiO$_2$, 80 mg of AIBN as the initiator, 10 mmol of EDMA as crosslinker were mixed in above solution and polymerized at 60 °C for 24 h under nitrogen protection. After the polymerization, the polymers were washed with the mixture of methanol / acetic acid (9:1, v/v) several times under ultrasound, until that the template molecule could not be detected.

The corresponding non-imprinted polymers (NIPs) were prepared in a similar manner as above, except without the addition of 2,4,6-TCP. For comparing, MIPs without GO (CdTe@SiO$_2$-MIPs) were prepared using the same procedure as the MIPs except without adding GO.
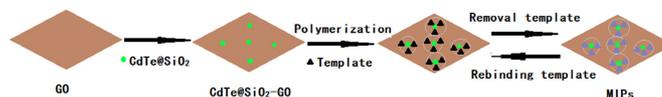
Fig. 1. Schematic of MIPs preparation.

2.3. Apparatus

Scanning electron microscope (SEM) images were carried out using a Japan HITACHI S-4300 scanning electron microscope. The X-ray diffraction (XRD) patterns were measured on a German Bruker D8-FOCUS X-Ray Diffraction. Morphological observation of the polymer particles was performed with a Japan SITACHI H-7650 transmission electron microscopy (TEM). Fluorescence spectra were collected on a Japan SHIMADZU RF-5301 spectrofluorimeter. Raman spectroscopy was recorded with Raman spectrometer (Jobin Yvon HR 800, with laser excitation at 457.9 nm). Thermo gravimetric analysis (TGA) was carried out with a German Netzsch STA 449F3 DSC-TGA. Ultraviolet-visible (UV-vis) absorption spectra were recorded on TU-1901 double beams UV-vis spectrophotometer (Purkinje General instument Co.,Ltd., China). The fluorescence microscopy digital images of the particles were acquired by using the inverted fluorescence microscope (Carl Zeiss, Germany). HPLC analysis was performed on the Dalian Elite P230 series HPLC system equipped with a UV–vis detector.

2.4. Incubation time test

The same amount of MIPs, CdTe@SiO$_2$-MIPs and NIPs particles were dispersed into 20 mL of 2,4,6-TCP solution (35 umol L^{-1}), respectively. The suspension was stirred under room temperature for different periods of time. The incubated solution was taken out and the fluorescence spectra and UV-vis absorption spectra were carried out. The amount of adsorbed 2,4,6-TCP can be determined by the difference in the concentration before and after the adsorption. The adsorption capacity (Q$_t$, expressed in units of umol g^{-1}) of the 2,4,6-TCP bound to MIPs was calculated by

$$Q_t = (C_0 - C_t) V / W \qquad (1)$$

where C_0 and C_t (umol L^{-1}) are the initial concentration and the residual concentration of 2,4,6-TCP, respectively, V (mL) is the volume of the initial solution, and W (g) is the weight of the polymers.

2.5. Fluorescence measurement

20 mL of MIPs or NIPs suspensions (0.05 mg mL^{-1}) and different amount of 2,4,6 TCP were mixed and stirred under room temperature for 15 min. The fluorescence intensity of suspensions was measured after stirring under room temperature for 15 min. The fluorescence intensity was recorded at 560 nm with the excitation of 470 nm and the slit widths of excitation and emission were both 10 nm.

2.6. Selectivity recognition experiments

To measure the selectivity recognition of MIPs for 2,4,6-TCP, the recognition for 4-CP and Phe were performed according to the procedure of the above experiment, namely, fluorescence measurements.

2.7. Preparation of the MISPE and chromatographic conditions

100 mg of MIPs particles were packed into an empty column served as MISPE. The MISPE cartridge was conditioned with 10 mL of methanol and 10 mL of water successively. Water sample was passed through the cartridge at 1.5 - 2.0 mL min^{-1} using a suction system. After the extracts were cleaned up by 2 mL of methanol, 25 min dryness of the cartridge was operated by vacuum to avoid incomplete fraction. Then the extracts were eluted with a solution of acetonitrile/acetic acid (acetonitrile : acetic acid = 99.0 : 1.0, v/v). Finally the obtained extract solution was blown down under nitrogen to final volume of 0.5 mL for subsequent HPLC analysis. All compounds were detected at 294 nm under the optimum HPLC mobile phase (methanol：HAc ：water = 80 : 0.3 : 19.7) at a flow rate of 0.5 mL min^{-1}.

3. Results and discussion

3.1. Characterizations

The TEM image of GO is shown in Fig. 2a. As can be seen in the figure, GO is ribbon-like with wrinkles at the edge suggesting GO sheet was successfully exfoliated. The thin GO nanosheets provides large surface area for the assembly of the CdTe@SiO$_2$ and MIPs on the surface. In Fig. 2b and c, SEM was employed to observe the morphologies of MIPs and NIPs. The surface of MIPs was rougher than that of NIPs, despite their similar physicochemical properties, which may indicate the surface of MIPs had more cavities than that of NIPs owning to imprinted sites were left after the removal of template molecules from MIPs.
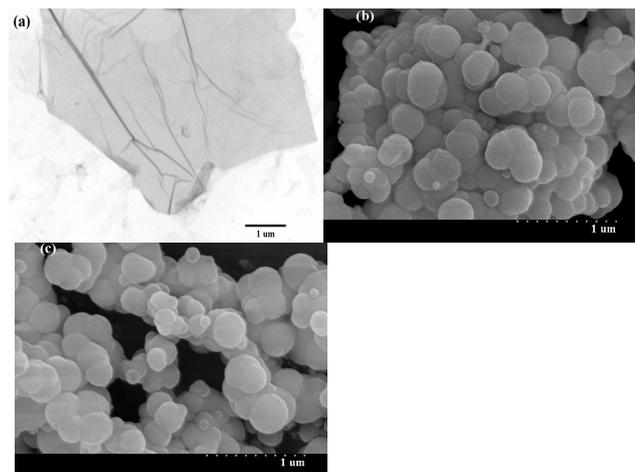
Fig. 2. TEM image of GO (a). SEM images of MIPs (b) and NIPs (c).

The XRD patterns of GO, CdTe and MIPs are shown in Fig. 3. As shown in Fig. 3 curve a, a characteristic peak around 11° is assigned to the (002) crystal of GO. In Fig. 3 curve b, the peak positions at corresponding 2θ value are indexed as (111), (220), (311) indicating that a cubic sphalerite structure of CdTe has been synthesized. In Fig. 3 curve c, the characteristic peaks of

CdTe and Fe$_3$O$_4$ are observed and the peak positions are unchanged. The faint diffraction peak of GO, which still exists in the XRD pattern, shows that a small quantity of GO was not exfoliated thoroughly [32]. The results suggested the phase of GO and CdTe was unchanged in the MIPs composite.
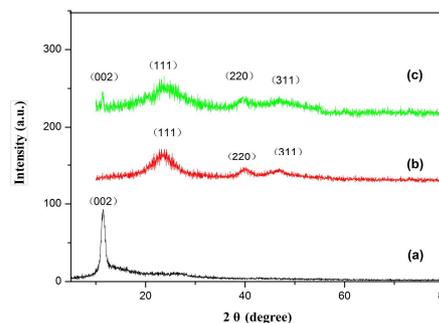
Fig. 3. XRD patterns of GO (a) CdTe QDs (b) and MIPs (c).

Fig.4 shows TGA curves of CdTe@SiO$_2$-GO and MIPs. For MIPs, the loss of weight below 120 °C can be ascribed to the loss of the residual or adsorbed solvent. Then the slight loss of weight occurs from 120 to 380 °C, which may be assigned to the decomposition and vaporization of various oxygen-containing functional groups [33]. After that, the abrupt loss of weight occurs from 300 °C to 550 °C, which may be assigned to the degradation of carbon skeleton of MIPs [34]. Moreover, it is evident that the total loss of weight of MIPs was much higher than the substrate CdTe@SiO$_2$-GO, which further suggested the successful synthesis of MIPs.
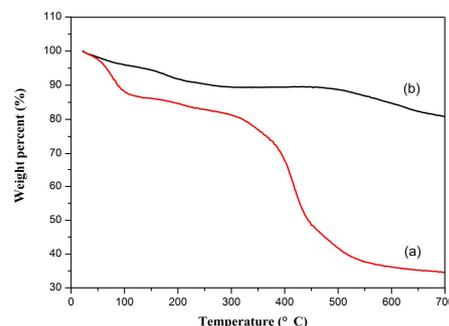
Fig. 4. TGA curves of MIPs (a) and CdTe@SiO$_2$-GO (b).

GO and MIPs were studied with Raman spectroscopic in Fig. 5. In Fig. 5 cure a, the D band (1338 cm^{-1}) and G band (1594 cm^{-1}) that are corresponding to originating from disordered carbon and sp^2 hybridized carbon respectively can be observed. Compared with that of GO, the peak position of MIPs does not shift but the enhanced radio of I(D) to I(G) can be found. Generally, the increasing ratio of I(D) to I(G) reflects the increasing of disorder form within the materials [28]. Thus the enhanced ratio for MIPs can be attributed to CdTe@SiO$_2$ with imprinted polymers film coating on GO, which lead to the increase of disorder in materials. These results further provided the evident for the successful synthesis of MIPs.
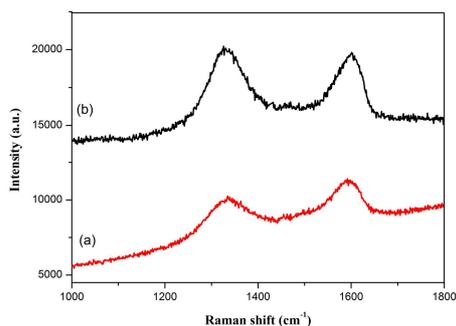
Fig. 5. Raman spectra of GO (a) and MIPs (b).

3.2. Fluorescence properties of MIPs

Fig. 6a shows the fluorescence microscopy image of MIPs showing bright green fluorescence, which suggests that the fluorescence intensity of MIPs was high. It provides a necessary prerequisite for fluorescence analysis. The photoluminescence emission from the composite was also studied (Fig. 6b). The fluorescence intensity of MIPs partly decreased during the preparation process in comparison with that of the CdTe QDs. That was consistent with the previous report that a single charge close to the QDs surface could generate an electric field, which was sufficiently large to cause fluorescence quenching [35]. The fluorescence intensity of MIPs was restored almost to that of the NIPs, which indicated that the templates were completely removed from the recognition cavities in the MIPs. Moreover, the result suggested that the MIPs possessed fast adsorption and desorption kinetics, which actually facilitated the application for the rapid and simple quantification of templates[36].
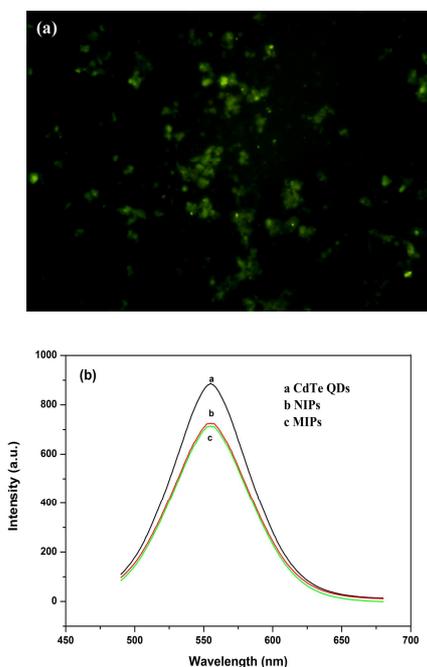
Fig. 6. Fluorescence microscopy image (a) of MIPs. Fluorescence emission spectra (b) of CdTe QDs, NIPs and MIPs.

3.3. Binding kinetics

A binding kinetic study had been carried out for MIPs, NIPs and CdTe@SiO$_2$-MIPs to determine the rate of the adsorption (Fig. 7). This is an important consideration in the practical application of the polymers. After MIPs dispersing into 2,4,6-TCP solution, the fluorescence intensity of MIPs decreased rapidly with increasing time in the initial 10 min, after which the curve became flat (Fig. 7a). Therefore, the sensor had a rapid response speed for 2,4,6-TCP and the sensing rate of MIPs was larger than that of CdTe@SiO$_2$-MIPs. The same result can be seen in Fig. 7b, during the initial adsorption process of MIPs, the presence of a large amount of empty, high-affinity binding sites on the surface of MIPs enabled template 2,4,6-TCP to easily bind to them with less resistance, therefore, the adsorption kinetic of MIPs showed rapid increase in the initial time. After that, with time increasing, when adsorbed 2,4,6-TCP occupied most of the binding sites, the adsorption rate slowed down and eventually reached adsorption equilibrium. MIPs need only 10 min to reach adsorption equilibrium for 2,4,6-TCP templates. Therefore, in our case, 2,4,6-TCP molecules reached the surface imprinting cavities of MIPs easily and took less time to reach adsorption saturation, which implies that MIPs has the property of good mass transport and thus overcomes some drawbacks of traditional packing imprinted materials. The changes in fluorescence intensity for MIPs were much more significant than that for CdTe@SiO$_2$-MIPs and NIPs, and the adsorption capacity of MIPs (600 umol g^{-1}) was much higher than that of CdTe@SiO$_2$-MIPs and NIPs. These results confirmed that the combination of MIPs with GO could improve fluorescence response speed and adsorption capacity. It may be suggested that lots of CdTe@SiO$_2$ were situated on the GO surface, and the imprinted binding sites were exposed on that hybrid surface after molecular imprinting process. Thus MIPs has more binding sites and better site accessibility to increase mass transfer rate and adsorption capacity [37]. As NIPs lacked the imprinting process, the functional groups were distributed randomly, which resulted in low adsorption ability. Hence, nonspecific adsorption of 2,4,6-TCP was observed. MIPs adsorbed more template 2,4,6-TCP than NIPs due to the imprinting effect.
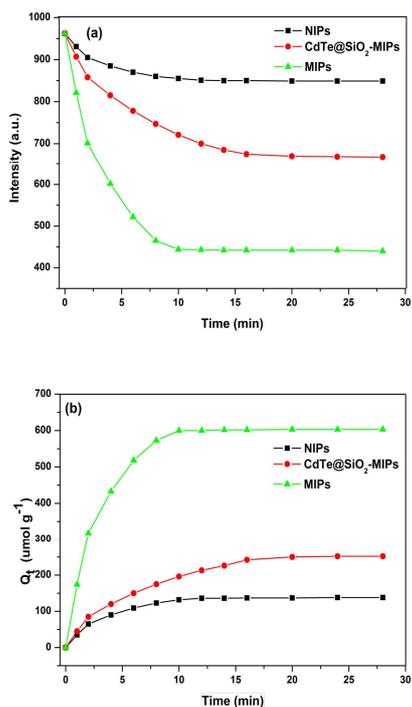
Fig. 7. Fluorescence response time (a) and UV detection (b) of different polymers for 2,4,6-TCP.

3.4. Optosensing of 2,4,6-TCP by MIPs

Typical spectrofluorimetric titration spectra of MIPs and NIPs with 2,4,6-TCP are presented in Fig. 8a and Fig. 8b. The fluorescence intensity of the composites gradually decreased with the increase of the 2,4,6-TCP concentration. However, the fluorescence quenching was much more noticeable with the MIPs than with the NIPs. Generally, the fluorescence quenching depends on the adsorptive affinity of the composites and analytes. In the case of MIPs, the fluorescence quenching was mainly achieved by the affinity of the imprinted cavities for the template because of the specific interactions. The relationship between the fluorescence intensity and the concentration of 2,4,6-TCP can be described by the Stern-Volmer equation:

$$I_0 / I = 1 + K_{sv}[Q] \tag{2}$$

I_0 and I are the fluorescence intensity in the absence and presence of template, respectively, K_{sv} is the Stern-Volmer constant, and $[Q]$ is the quencher concentration. Fig.8c is plotted by the Stern-Volmer equation analysis for the MIPs and NIPs with 2,4,6-TCP, respectively. The K_{sv} of the MIPs was much larger than that of NIPs, which indicated that MIPs could greatly enhance the quenching efficiency, and enlarge the spectral sensitivity to 2,4,6-TCP. For MIPs the linear range was 0.2- 40 μ mol L^{-1}, with a correlation coefficient of 0.9994. The detection limit, which was calculated as the concentration of 2,4,6-TCP for which the quenched amount was three times the standard deviation of the blank signal, of 0.18 μ mol L^{-1} was attained. The precision for the three-replicate detection of 2,4,6-TCP was 2.5% (relative standard deviation, RSD). Thus the sensor was demonstrated to be highly sensitive and reliable for the detection of 2,4,6-TCP. The developed method was simple, effective and time-saving without expensive instrument.
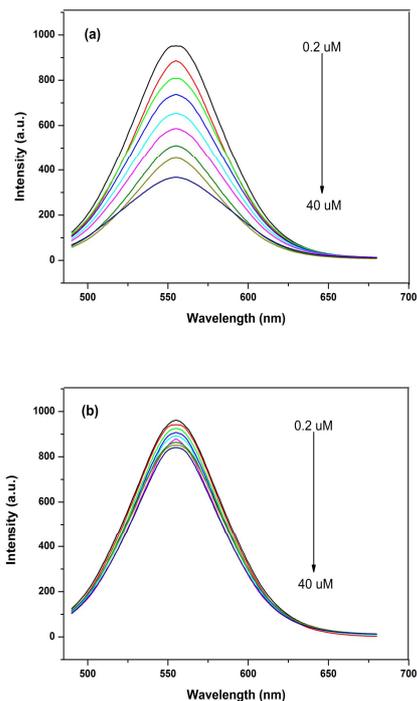
Fig. 8. Fluorescence emission spectra of MIPs (a) and NIPs (b) with addition of the indicated concentration of 2,4,6-TCP solution. Stern-Volmer plots (c) from MIPs and NIPs with 2,4,6-TCP.

3.5. Selectivity of the MIPs

The selectivity of the MIPs was investigated using 4-CP and Phe as the structural analogs of the template 2,4,6-TCP (Fig. 9). The K_{sv} of the MIPs for 2,4,6-TCP was higher than that for 4-CP and Phe. The NIPs showed similar selectivity for 2,4,6-TCP as for 4-CP and Phe. This phenomenon could be explained as follows: in the synthesis process, many specific recognition sites with respect to the template were generated on the surface of MIPs, and these sites were complementary in shape, size, and spatial arrangement to 2,4,6-TCP, thus 2,4,6-TCP molecules had advantage in occupying the binding sites over the other analogs. The template 2,4,6-TCP could be bound strongly to the MIPs and cause significant changes in the fluorescence intensity. For NIPs fluorescence quenching of all the analogs and 2,4,6-TCP was quite close and very little,

suggesting that the NIPs could not effectively bind 2,4,6-TCP as well as its analogs. However, it is well known that the imprinting factor (α) is an important index to evaluate the selectivity of the imprinted materials, which is calculated as the ratio of the K_{sv} value of the MIPs to that of NIPs. Under optimum conditions, the imprinting factor was 4.60, indicating that the MIPs had much better selectivity than the NIPs. Furthermore, it is indicated that, the MIPs with high selectivity and sensing specificity can be applied for the direct detection of 2,4,6-TCP from complex matrices without separation.
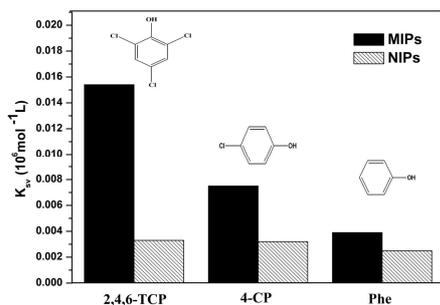
Fig. 9. Quenching constant of MIPs and NIPs by different kinds of phenols.

3.6. Application to water sample analysis.

Water sampels	Added (umol L^{-1})			Founded (umol L^{-1})	Recovery (%)	RSD (%, n=6)
	2,4,6-TCP	4-CP	Phe			
Tap water	2	0	0	1.87	93.5	2.4
	4	0	0	3.81	95.2	2.1
	6	0	0	5.53	92.1	2.5
Labor Lake water	2	4	4	2.15	107.5	3.8
	6	8	8	6.35	105.8	3.1
Nenjiang River water	2	4	4	2.13	106.5	3.5
	6	8	8	6.32	105.3	3.2

Table 1 Detection of 2,4,6-TCP in real water samples by MIPs-based photoluminescence sensor

To evaluate the accuracy and potential application of the method, the developed sensor based on MIPs was applied to determine 2,4,6-TCP in water samples (Table 1). The water samples were collected from the local city. As no 2,4,6-TCP in the collected water samples were detectable by the proposed method, a recovery study was carried out on the samples spiked with 2,4,6-TCP (2 - 6 umol L^{-1}) to evaluate the developed method. Lake and river water samples spiked by a mixture of 2,4,6-TCP, 4-CP and Phe were also analyzed for 2,4,6-TCP. The concentrations of 2,4,6-TCP in the spiked samples determined by the developed method were in good agreement with those of 2,4,6-TCP added. For each sample, six parallel

experiments were conducted, and the recoveries were from 92.1 % to 107.5 % with the RSD ranging from 2.1 % to 3.8 %, demonstrating the potential applicability of MIPs for simple and selective determination of 2,4,6-TCP in real water samples.

3.7. MISPE－HPLC determination of trace 2,4,6-TCP

The applicability of the MIPs to MISPE-HPLC determination of trace 2,4,6-TCP was evaluated. The sample volume and sample loading flow rate were optimized to achieve good sensitivity and precision. When the sample (10 ug L^{-1}) volume were 2, 4, 6, 8, 10, 15 mL, the recoveries obtained were 90%, 92%, 90%, 91%, 92%, 75%, respectively. The acceptable recovery was shown when sample volumes increased to 10 mL, it seemed to be the tolerated volume for breakthrough. Thus, 10 mL was used as the optimal sample volume. Generally, higher sample loading flow rate leads to the decrease of interaction time between the analytes and the sorbent, and the analytes recovery decreases. Too low flow rate causes low efficiency. However it was discovered that the recovery of 2,4,6-TCP decreased slightly (about 3%) as the flow rate increased from 0.4 to 1.0 mL min^{-1}, decreased noticeable as the sample loading flow rate increased from 1.0 to 2.0 mL min^{-1}. Consequently, sample loading flow rate of 1.0 mL min^{-1} was selected. These results also indicated that the kinetics for the adsorption of 2,4,6-TCP by MIPs was very fast. Thus under the optimized conditions of MISPE-HPLC, the calibration graph was linear with a correlation coefficient of 0.9992 in the concentration range of 0.02 - 2.5 umol L^{-1}. The enrichment factor obtained by comparing the slopes of the linear portion of the calibration curves before and after the extraction was 460. A detection limit (S/N = 3) of 0.25 ng mL^{-1} was achieved and RSD was 5.5% at a concentration of 1.0 umol L^{-1} (n = 6).

Fig. 10 chromatogram (a) shows the chromatogram of direct infection of 20 uL the standard mixture solution containing 20 mg L^{-1} of 2,4,6-TCP, 4-CP, Phe. Good baseline separation was obtained for them without SPE procedure. Fig. 10 chromatogram (b) shows the chromatogram of 10 mL standard mixture solution containing 20 ug L^{-1} of 2,4,6-TCP, 4-CP, Phe after eluting from the imprinted cartridge. The peak of 2,4,6-TCP increased greatly in chromatogram (b) indicating that 2,4,6-TCP was selectively extracted onto the imprinted sorbent. Moreover, it was suggested the MIPSPE not only had ability of high selectivity recognition for 2,4,6-TCP but also offered cleanup and enrichment effects for the sample. Thus, it was indicated this method could be used to selectively detect some trace-level 2,4,6-TCP from the environmental water.
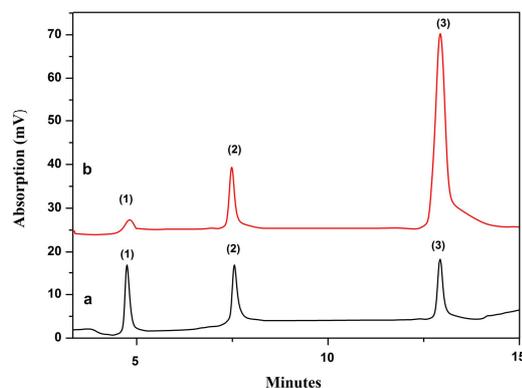
Fig.10. Chromatograms of standard mixture solution containing 20 mg L^{-1} of each different kinds phenols (a) and 10 mL standard mixture solution containing 20 ug L^{-1} of each different kinds phenols after SPE procedure(b). Peak identifications: (1) Phe, (2) 4-CP, (3) 2,4,6-TCP.

4. Conclusion

In this work, the synthesized composite integrating the advantages of high selectivity of molecular imprinting and strong fluorescence property of CdTe QDs were prepared. Moreover, owning to the use of GO as the substrate in MIPs, the resultant MIPs displayed fast sensing rate and high adsorption capacity. Furthermore, on the one hand, MIPs were successfully applied for direct, sensitive, and selective fluorescence detection of 2,4,6-TCP in water, independent of sample pretreatment, expensive instruments, as well as time consuming analysis processes. On the other hand, the MIPs used as the MISPE followed by HPLC for enrichment and analysis of trace 2,4,6-TCP showed good selectivity and enrichment efficiency. At last the sensing strategy in this work established the basis for selective separation and rapid detection of 2,4,6-TCP from complicated matrices and developed attractive perspectives for many other analytes.

Acknowledgements

Notes and references

a Department of Chemistry, Harbin Institute of Technology, Harbin 150090, China

b College of Chemistry and Chemical Engineering, Qiqihar University, Qiqihar 161006, China

c State Key Lab of Urban Water Resource and Environment, Harbin Institute of Technology, Harbin 150090, China

d Qiqihar Environmental Monitoring Central Station, Qiqihar 161005, China

E-mail: lixin@hit.edu.cn

1. S. Maddila, V.D. Dasireddy, E.O. Oseghe, S.B. Jonnalagadda, *Appl. Catal., B,* 2013, **142-143**, 129-141.
[2] G.D. Díaz, M.C.B. López, *J. Mol. Catal. A: Chem.,* 2012, **353-354**, 117-121.
[3] J.T. Huang, L. Alquier, J.P. Kaisa, G. Reed, T. Gilmor, G. Vas, *J. Chromatogr. A,* 2012, **1262**, 196-204.
[4] Q.H. Zeng, S. Peng, M. Liu, Z.J. Song, X.K. Wang, X. Zhang, S. Hong, *Chem. Eng. J. ,* 2013, **230,** 202-209.
[5] H.H. Ji, F. Chang, X.F. Hua, W. Qin , J.W. Shen, *Chem. Eng. J.,* 2013, **218,** 183-190.
[6] M. Jin, X. Chen, B. Pan, *J. Liq. Chromatogr. Related Technol.,* 2006, **29**, 1369–1380.
[7] FD. Wei, Y.Z. Wu, G.H. Xu, Y.K. Gao, J. Yang, L.P. Liu, P. Zhou, Q. Hu, *Analyst*, 2014, **139**, 5785-5792.
[8] T.C. Zhou, L. Jørgensen, M.A. Mattebjerg, I.S. Chronakis, L. Ye, *RSC Adv.,* 2014, **4**, 30292-30299.
[9] X.P. Jia, M.L. Xu, Y.Z. Wang, D. Ran, S. Yang, M. Zhang, *Analyst,* 2013, **138**, 651-658.
[10] J. Ji, X.L. Sun, X.M. Tian, Z.J. Li, Y.Z. Zhang, *Anal. Lett.,* 2013, **46**, 969-981.
[11] X. Xue, Q. Wei, D. Wu, *Electrochim. Acta,* 2014, **116**, 366-371.
[12] D. Cleland, G.D. Olsson, B.C.G. Karlsson, *Org. biomol. Chem.,* 2014, **12**, 844-853.
[13] H.L. Liu, G.Z. Fang, H.D. Zhu, C.M. Li, C.C. Liu, S. Wang**,** *Biosens. Bioelectron.,* 2013, **47**, 127-132.
[14] S. Ying, S. Cui, W. Wang, J. Feng, *J. Chen, J. Lumin.,* 2014, **145**, 575-581.
[15] Q. Mu, H. Xu, Y. Li, *Analyst* , 2014, **139**, 93-98.
[16] M. Zorn, W.K. Bae, J.K wak, H. Lee, C. Lee, R. Zentel, K. Char, *ACS Nano.,* 2009, **3**, 1063-1068.
[17] H. Liu, F. G, S. Wang, *Biosens. Bioelectron.,* 2014, **55**, 127-132.
[18] L. Tan, C. Kang, S.Y. Xu, Y.W. Tang, *Biosens. Bioelectron.,* 2013, **48**, 216–223.
[19] Y. Q. Yang, X.W. He, Y.Z. Wang, *Biosens. Bioelectron.,* 2014, **54**, 266-272.
[20] S. Han, X. Li, Y. Wang, C. Su, *Anal. Methods,* 2014, **6**, 2855-2861.
[21] B.T Huy, M.H. Seo, X. Zhang, Y. I. Lee, *Biosens. Bioelectron.,* 2014, **57**, 310-316.
[22] H.F. Wang, Y. He, T.R. Ji, X.P. Yan, *Anal. Chem.,* 2009, **81**, 1615-162.
[23] Y.B. Zeng, Y.Z. LeiKong, T.Z. Zhou, G.Y. Shi, *Biosens. Bioelectron.* 45 (2013) 25-33.
[24] Y. Liu, L.H. Zhu, Z.H. Luo, H.Q. Tang, *Sens. Actuators, B,* 2013, **185**, 438-444.
[25] Y. Liu, L.H. Zhu, Y.Y. Zhang, H.Q. Tang, *Sensor Actuat. B Chem.,* 2012, **171**, 1151-1158.
[26] Y. Li , X. Li , C.K. Dong, J.Y. Qi, X.J. Han, *Carbon,* 2010, **48**, 3427-3433.
[27] H.M. Qiu, C.N. Luo, M. Sun, F.G. Lu, L.L. Fan, X.J. Li, *Carbon,* 2012, **50**, 4052-4060.
[28] S.F. Xu, H.Z. Lu, X.W. Zheng, L.X. Chen, *J. Mater. Chem. C,* 2013, **1**, 4406-4422.
[29] L.X. Chen, S.F. Xu, J.H. Li, *Chem. Soc. Rev.,* 2011, **40**, 2922-2942.
[30] X.Y. Yang, X.Y. Zhang, Y.F, Ma, Y. Huang, Y.S, Wang, Y.S. Chen, *J. Mater. Chem.,* 2009, **19**, 2710-2714.
[31] S.G. Ge, C.C. Zhang, Y.N. Zhu, J.H. Yu, S.S. Zhang, *Analyst,* 2010, **135**, 111-115.
[32] Y.J. Yao, S.D. Miao, S.Z. Liu, L.P. Ma, H.Q. Sun, S.B. Wang, *Chem. Eng. J.,* 2012, **184**, 326-332.
[33] Y.H. Song, Z.F. He, H.Q. Hou, X.L. Wang, L. Wang, *Electrochim. Acta,* 2012, **71**, 58-65.
[34] Y.B. Zeng, Y. Zhou, L. Kong, T.S. Zhou, G.Y. Shi, *Biosens. Bioelectron.,* 2013, **45**, 25-33.
[35] S.F. Xu, H.Z. Lu, J.H. Li, X.L. Song, A.X. Wang, L.X. Chen, S.B. Han, *Appl. Mater. Interfaces,* 2013, **5**, 8146-8154.
[36] Y.Y. Zhao, Y.X. Ma, H. Li, L.Y. Wang, *Anal. Chem.,* 2012, **84**, 386-395.
[37] P.S. Sharma, M. Dabrowski, F. D'Souza, W. Kutner, *Trace Trends Anal.Chem.,* 2013, **51**, 146-157.

RSC Advances Accepted Manuscript